Atomic effects in heavy-ion elastic scattering

J. M. Casandjian,[1,*] R. Lichtenthäler,[2] W. Mittig,[1] A. Lépine-Szily,[2] A. C. C. Villari,[1] G. Auger,[1] R. Beunard,[1] L. Bianchi,[1] M. E. Brandan,[3] J. L. Ciffre,[1] A. Cunsolo,[4] A. Foti,[4] A. Menchaca-Rocha,[3] N. A. Orr,[5] E. Plagnol,[6] R. H. Siemssen,[7] and J. P. Wieleczko[1]

[1]*GANIL, B.P. 5027, 14021 Caen Cedex, France*

[2]*Instituto de Física da Universidade de São Paulo, C.P. 66318, 05389-970, São Paulo, S.P., Brazil*

[3]*Instituto de Física UNAM, A.P. 20-364, 01000 DF, Mexico*

[4]*Dipartimento di Fisica and INFN – Sez. CT, 95129 Catania, Italy*

[5]*LPC-ISMRA, Bld du Marechal Juin, 14050 Caen, France*

[6]*IPN Orsay, B.P. 1, 91406 Orsay, France*

[7]*KVI, 9747 AA Groningen, The Netherlands*

(Received 26 February 1997)

Angular distributions of a ^{208}Pb beam on ^{208}Pb thin targets at very small angles were measured. The shape of the experimental distribution is not Gaussian, indicating a plural scattering regime rather than multiple scattering. The distribution was well reproduced by a Monte Carlo simulation of the straggling process. For the first time we observed and quantified the influence of the production of electrons during the scattering. This effect was observed in the angular correlation of the scattered ^{208}Pb nuclei detected in kinematic coincidence and also in the limiting angle of the ^{208}Pb scattered in a ^{107,109}Ag target. This effect introduces a spread in the scattered angle which is of the same order of magnitude as the angular straggling. [S0556-2813(97)01709-3]

PACS number(s): 25.70.Bc, 34.50.−s, 25.70.−z, 24.10.Lx

I. INTRODUCTION

Atomic effects have a wide range of contributions to nuclear physics. One of the most investigated is angular straggling due to its strong contribution to the resolution of an experiment. A good comprehension of angular straggling is important for activities related to ion implantation or penetration phenomena such as in medical applications. It is also a method to study the interatomic potential and electronic stopping cross section [1]. This increasing interest motivated us to study the angular straggling with the very heavy ^{208}Pb-^{208}Pb and ^{208}Pb-^{107,109}Ag systems at energies around the Coulomb barrier where experimental data were still missing.

The influence of the surrounding electrons during the scattering cannot be simply reduced to a modification of the interatomic potential. During a collision of two heavy ions at energies below the Coulomb barrier, the formation of a superheavy electronic quasimolecule is expected. The idea that quasimolecular states could be created during the scattering at low energies dates back to the 1930s [2,3], as well as the first experimental evidence [4]. In 1972 Saris *et al.* [5] observed for the first time the x-ray emission induced by nonadiabatic rearrangement in the electronic cloud of a quasimolecule. Meyerhof *et al.* [6] observed the same phenomenon for the ^{208}Pb-^{208}Pb system at 4.2 MeV/nucleon. One of the most interesting features accompanying quasimolecule formation is the production of energetic electrons. The production of these δ electrons is due to the presence of an intense Coulomb field created by the charge of both nuclei which induces a drastic increase of the binding energies and the momentum of the innermost electrons [7] and favors their ejection. The spectroscopy of δ electrons has been intensively studied to extract information about electron binding energies, nuclear delay times, or spontaneous positron emission [7], but, although the influence of a quasimolecular potential on the scattering angle has been suggested [8], the influence of electron production on the scattering angle and on angular straggling has never been investigated.

We performed such studies during an experiment in which the angular position of the ^{208}Pb-^{208}Pb elastic scattering cross-section oscillations was measured with an absolute precision of a few millidegrees [9,10].

II. EXPERIMENTAL ARRANGEMENT

The experiment was performed at GANIL using ^{208}Pb beams of several incident energies around 5 MeV/nucleon and ^{208}Pb targets of approximately 10, 20, and 30 μg/cm^2 evaporated on 20-μg/cm^2 carbon backings. The detection system (Fig. 1) consisted of two pairs of x-y drift chambers [11] at 30°-60° and 45°-45° working in kinematic coincidence. The angular aperture of the drift chambers was 6° in the horizontal plane (x) and 0.9° in the vertical plane (y) for the 30°-60° pair and 0.9° in x and y for the 45°-45° pair. At zero degrees there was a beam scanner consisting of 47 wires disposed horizontally and vertically separated by 0.5 mm. All the detectors, the beam scanner, and the target were placed on a circle of 7 m diameter and the beam was focused on the beam scanner downstream of the target during the experiment. In this way, all events occurring in the detector at a given position correspond to the same scattering angle, independent of the point where the scattering took place in the target or of the angle of incidence of the beam. Before each measurement, the beam was focused on the central wire of the beam scanner without target and in this situation only a few wires were hit. With the target in position there is a

*Present address: Nuclear Physics Laboratory, University of Washington, Seattle, WA 98195.

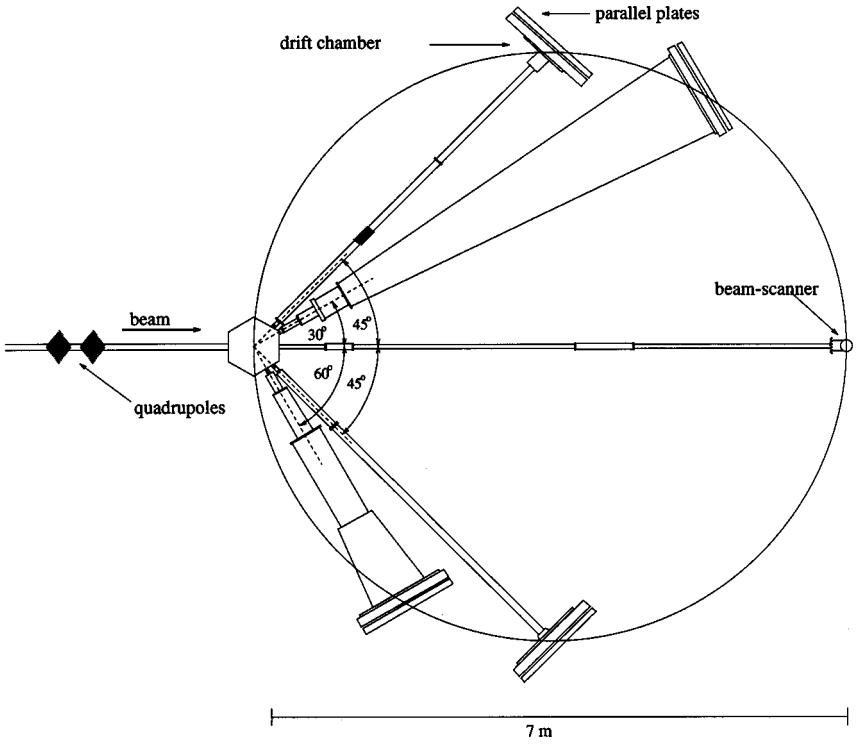

FIG. 1. Experimental setup mounted at GANIL. The beam was focused on a beam scanner situated 7 m downstream from the target. The nuclei scattered were detected in coincidence in four x-y drift chambers situated at 30°-60° and 45°-45° on a circle passing through the target and the beam scanner.

Lorentzian-like intensity distribution in the beam scanner due to the angular straggling (Fig. 2). The effect of the angular straggling is also observed in the angular correlation $(\Theta_1+\Theta_2)$ of the scattered particles detected in the x-y drift chambers which presented a distribution around $\Theta_{\rm lab}=89.9°$ (it is not exactly 90° due to the relativistic kinematics). During the entire experiment the incident beam energy was measured with a precision of $\Delta E/E\leqslant 10^{-4}$ by a time-of-flight technique [12]. The absolute angular calibration was determined by measuring all distances between the components of the experimental arrangement using INVAR wires calibrated with the interferometric facility of the CEA/Saclay. The final angular precision obtained by this method was of the order of a millidegree. The relative angular calibration of all position-sensitive detectors was performed at the beginning and at the end of the experiment using carefully aligned slotted plates in front of the detectors. As an independent absolute angular measurement method, we used natural Ag targets composed of 51.8% ^{107}Ag and 48.2% ^{109}Ag. This permitted the observation of the kinematic limiting angles of the ^{208}Pb-^{107}Ag and ^{208}Pb-^{109}Ag scattering in the drift chamber centered at 30°. The 30° x spectrum shows an increasing yield with a cutoff in the limiting angles. The width of this cutoff is due to angular straggling in the target and to the production of δ electrons.

III. ANALYSIS: MONTE CARLO SIMULATION

In order to analyze the experimental distributions a program was written which uses a Monte Carlo method to simulate the straggling of the incident nuclei through the target. We assumed that each scattering center occupies a sphere of radius r_0, half of the distance between immediately neighboring atoms $r_0\simeq 1/2N^{-1/3}$, where N is the number of atoms per unit volume. The average number of collisions in a target of thickness t is then $n=\pi r_0^2 Nt$. In order to choose the scattering angle in each collision it is necessary to know the differential cross section which is determined by the shielded Coulomb potential between the incident nucleus and the target nucleus. For heavy nuclei a reasonable description can be obtained by the Thomas-Fermi potential [13–15]

$$V(r)=\frac{Z_1Z_2e^2}{r}\chi\left(\frac{r}{a}\right),$$

where $a=0.885a_0/(Z_1^{2/3}+Z_2^{2/3})^{1/2}$ is a screening parameter, $a_0=0.529\times 10^{-8}$ cm is the Bohr radius, Z_1 and Z_2 are the atomic numbers of the colliding nuclei, and $\chi(r)$ a function representing the screening of the electrons. The function χ corresponding to the Thomas-Fermi potential is given in tabulated form, for instance, in Ref. [16]. The cross section for each atomic scattering has been deduced by Lindhard, Nielsen, and Scharff [17]. They showed that the dependence of the cross section on the energy and on the scattering angle can be reduced to a dependence on a dimensionless quantity $\eta=\varepsilon\sin(\theta_{\rm lab}/2)$ where $\varepsilon=aE_{\rm lab}/(Z_1Z_2e^2)$. The differential cross section can be obtained from classical mechanics:

$$\frac{d\sigma}{d\eta}=\pi a^2\frac{f(\eta)}{\eta^2}, \tag{1}$$

where f is given by a numerical table in Ref. [17].

A variable η was sorted following the probability obtained from Eq. (1) after each scattering and transformed into a horizontal plane scattering angle. The azimuthal angle was randomly chosen between 0 and 2π in order to obtain for each scattering the scattering angle θ_i. Each angle was projected and added to the previous one until n scatterings were obtained.

The beam profile calculated with this simulation is compared in Fig. 2 with the one obtained experimentally in the

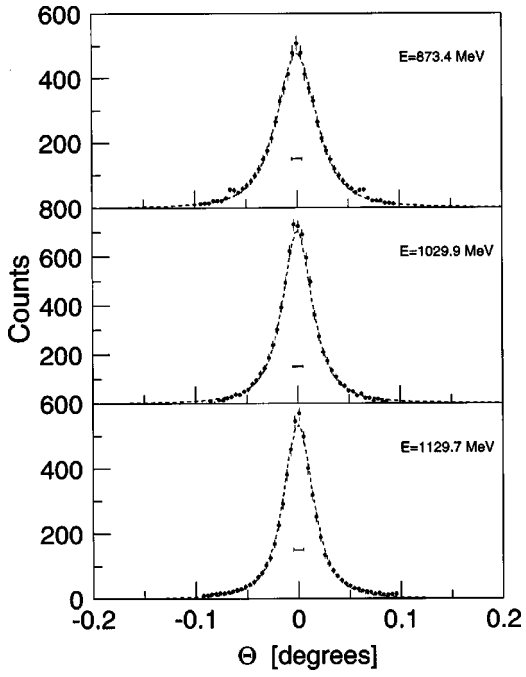

FIG. 2. Profile of the beam at 0° with a ^{107,109}Ag target obtained with the beam scanner for three incident beam energies. The points represent the intensities on the wires of the beam scanner. The dashed curves are the results of the Monte Carlo simulation. The horizontal bar at the center of the peaks indicates the full width at half maximum observed without a target.

beam scanner as described below. This figure shows the profile of a ^{208}Pb beam after passing through a ^{107,109}Ag target plus a carbon layer, with the Ag layer facing the beam. Three different targets were used with nominal thickness of 40 μg/cm^2 of natural silver plus a carbon layer of 25 μg/cm^2 (10 and 25 μg/cm^2), respectively, at $E_{\rm lab}=873.4$ MeV (1029.9 and 1129.7 MeV). The points represent the intensity read on the beam-scanner wires versus the angular position of these wires. As can be seen the distribution is not Gaussian with a full width at half maximum (FWHM) of about 0.04°, depending on the energy and the target used. The fact that the distribution is not Gaussian is expected for plural scattering [18]. The solid lines in Fig. 2 show the results of the Monte Carlo simulation for the three beam energies. The calculation was normalized to the experimental data. The thickness of the targets was adjusted in the simulation to fit the data. We used the nominal thickness of the carbon backing and the following thicknesses of silver: 39, 41, and 38 μg/cm^2, respectively, for the three energies, which agrees with the nominal thickness within the uncertainty. A very good agreement between the experimental data and the simulation results is obtained. The angular straggling at 0° is thus perfectly reproduced in this approach in which the electrostatic potential is calculated with the Thomas-Fermi method.

IV. PRODUCTION OF δ ELECTRONS

As stated in the introduction, the energy loss during the scattering is expected to be due to the production of δ electrons. If the scattering angle is small, the distance of closest approach between the colliding nuclei is large and the energy of the emitted electrons is expected to be small. However, when the scattering angle is large ($\Theta=30°$) the distance of closest approach is small ($\simeq 25$ fm) making the sum total energy of the emitted electrons to be of the order of 1 MeV. Hence we expect to observe the effect of the δ electrons in the scattering angle distribution of the ^{208}Pb-^{208}Pb system and also in the spectrum of the limiting angle of the ^{208}Pb-^{107,109}Ag system. We have used a simple model to calculate the energy loss due to the emission of electrons during the ^{208}Pb-^{208}Pb scattering and to predict the subsequent change in the angle between the trajectories of the two lead nuclei. This angle, which we will now refer to as the folding angle, is given exactly by the relativistic kinematics but is reduced in the laboratory frame because of the energy loss due to the production of δ electrons. It is important to note that this energy loss is not the usual energy loss due to a succession of collisions with the electrons of the target atoms which is already taken into account in the incident beam energy but it is due to the emission of electrons in one nucleus-nucleus collision during the Rutherford scattering process. To quantify the accompanying change in angle we will first estimate the energy loss. Kankeleit [19] obtained by a perturbation calculation the electron emission probability during the scattering:

$$\frac{dP}{dE_{e^-}}=C\frac{1}{(E_{e^-}+\overline{E_B})^2}\exp\left(-2\frac{E_{e^-}+\overline{E_B}}{\hbar}\hat{t}\right), \qquad (2)$$

where E_{e^-} is the kinetic energy of the electrons, $\overline{E_B}$ their mean binding energy, C is a constant, and $\hat{t}$ is the characteristic collision time calculated with the trajectory eccentricity ε and the velocity at infinity v: $\hat{t}\simeq a/v(\varepsilon+1.6+0.449/\varepsilon)$.

The value of the normalization constant C and the mean binding energy corresponding to the ^{208}Pb-^{208}Pb system were obtained by fitting the results of the calculation of the two-center Dirac coupled equations performed by Ditzel [20]. These equations describe the relativistic behavior of an electron in the field created by two nuclei surrounded by electrons [21] and allow one to obtain the spectrum of the electrons emitted to the continuum. These predictions have already been successfully compared with experimental data [22].

From this fit we can deduce the electron emission probability dP/dE_{e^-} and the average number of electrons emitted in each scattering:

$$\overline{n}=\int_0^\infty \frac{dP}{dE_{e^-}}dE_{e^-}.$$

The average kinetic energy of these electrons is given by

$$\overline{E_{e^-}}=\frac{1}{\overline{n}}\int_0^\infty E_{e^-}\frac{dP}{dE_{e^-}}dE_{e^-}.$$

We obtained the result that around two and three electrons are ejected per scattering with an average kinetic energy between 45 and 85 keV and a binding energy between 120 and 190 keV depending on the incident beam energy and the impact parameter. The energy loss (Q) due to the emission of electrons can be deduced from these quantities:

TABLE I. Difference in degrees between the expected kinematic folding angle and the measured folding angle when the two lead nuclei are detected at 30°-60° and at 45°-45°. The uncertainty in this difference is 0.006°. The difference is due the production of electrons during the scattering process.

Energy [MeV]	$\theta_{\text{theor}}-\theta_{\text{expt}}$ (deg) 30°-60°	45°-45°
786.7	0.046	0.036
873.4	0.039	0.042
948.6	0.053	0.034
1029.9	0.047	0.040
1129.7	0.044	0.050
1306.4	0.054	0.039

$$Q=\int_0^{\infty}(E_{e^-}+\overline{E_B})\frac{dP}{dE_{e^-}}dE_{e^-}$$
$$=\overline{n}(\overline{E_{e^-}}+\overline{E_B}). \quad (3)$$

This expected energy loss was compared with the energy loss obtained experimentally by measuring the folding angle of the scattered ^{208}Pb nuclei in the 30°-60° and 45°-45° pairs of drift chambers. These two possibilities correspond to different impact parameters. Figure 4 presents the folding angle distribution measured in the 30°-60° configuration for two different beam energies. The difference between the expected relativistic kinematic folding angle and the measured folding angle is indicated in Table I. Using relativistic kinematics we transformed this difference into an equivalent energy loss in order to compare it with the energy loss Q of Eq. (3) predicted by the δ-electron production.

Figure 3 shows the absolute value of the expected (solid circle) and experimental (open circle) energy loss for five beam energies and for the 30°-60° and 45°-45° configurations versus the incident beam energy. The absolute value of Q obtained is slightly smaller than 1 MeV and increases with energy. The main contributions to the uncertainty of the folding angle and to the energy loss come from the absolute angular calibration of the drift chambers, the target position, and of the centroid of the folding angle distribution. The total uncertainties (quadratic sum of all these contributions) corresponding to the three detection angles are $\sigma_{\theta_{60}}=0.005°$, $\sigma_{\theta_{45}}=0.005°$, and $\sigma_{\theta_{30}}=0.003°$. The total uncertainty of the folding angle is the quadratic sum of the uncertainties associated with both angles: $\sigma_{\theta_{30\text{-}60}}=0.006°$ and $\sigma_{\theta_{45\text{-}45}}=0.006°$. This final uncertainty is equivalent to an uncertainty of 100 keV on the energy loss and is represented by the error bars of Fig. 3. In this figure we also present the energy loss expected by Eq. (3). The very good agreement obtained at 45°-45° and the good agreement at 30°-60° show that the emission of electrons during the scattering can explain the shift of approximately 0.05° (Table I) of the folding angle.

Other possible processes which could contribute to the energy loss are Coulomb excitation and bremsstrahlung radiation. The Coulomb excitation can be neglected since the high energy of the first excited state of ^{208}Pb and the discrete nature of the excitation make the discrimination of the inelastic peak possible within our experimental resolution. The dipole contribution of the bremsstrahlung radiation cancels because of the symmetry of the system. We performed a semiclassical calculation to obtain the energy loss due to the quadrupole contribution [23,24]. In contrast to the result of [25], we found that this contribution is of the order of a few hundreds of electron volts and therefore negligible. The difference between the result of [25] and ours could originate from a misprint in Ref. [24].

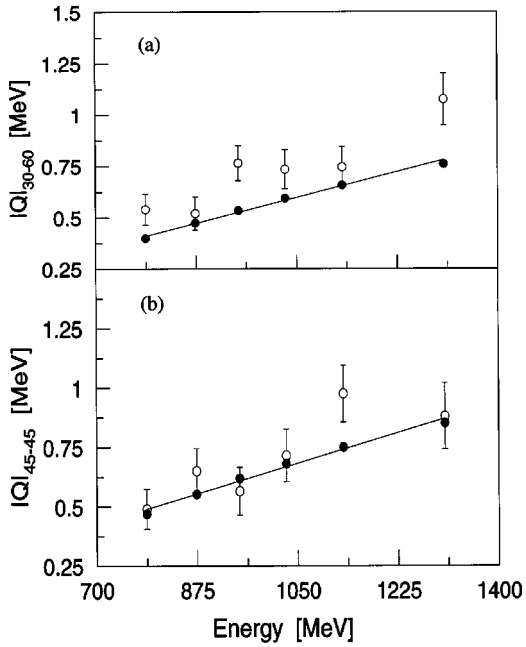

FIG. 3. Absolute value of the energy loss for the ^{208}Pb-^{208}Pb scattering at 30°-60° (a) and 45°-45° (b). The open points are the experimental data obtained by measuring precisely the folding angle. The solid circles are the results of a calculation in which the energy loss is due to the production of electrons during the scattering. The solid line is a guide to the eye.

Similar energy losses due to the emission of δ electrons were also observed by us for the ^{208}Pb-^{197}Au, ^{208}Pb-^{238}U, and ^{208}Pb-^{107,109}Ag systems. For the last mentioned system, the kinematics did not allow the detection in coincidence of the scattered nuclei. The energy loss was obtained by measuring the angular shift of the limiting angles observed at the 30°'s drift chamber. However, for these systems, in contrast to ^{208}Pb-^{208}Pb, Coulomb excitation gives a strong contribution in the energy loss. In the case of ^{208}Pb-^{238}U, about half of the energy loss is due to Coulomb excitation [26]. In this context, we will therefore not use these data.

The production of δ electrons is also most likely the cause of the unexplained deviation of the absolute angle observed in Ref. [27] with the ^{12}C-^{12}C system.

V. INFLUENCE OF δ-ELECTRON PRODUCTION ON THE WIDTH OF THE DISTRIBUTIONS

The width of the distributions observed in the folding angles measured at 30°-60° for the ^{208}Pb-^{208}Pb system (Fig. 4) and on the limiting angles at 30° for the ^{208}Pb-^{107,109}Ag scattering (Fig. 5) has two origins that must be considered: One is due to the angular straggling (plural scattering) that

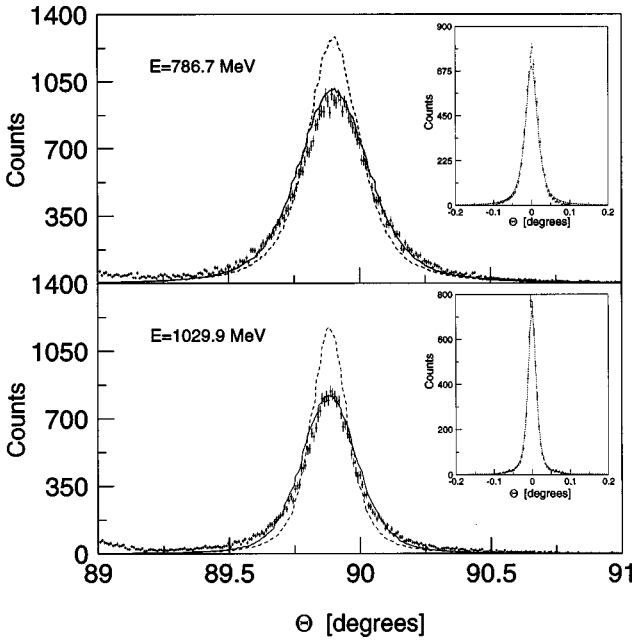

FIG. 4. Folding angle for the ^{208}Pb-^{208}Pb system for two beam energies. The points are the experimental data, and the dashed curves are the results of the simulation of the scattering without a fluctuation on the energy loss due to the fluctuation in the number of electrons emitted. When such a fluctuation is added we obtain the solid line. The insets represent the experimental and calculated beam profile at 0° for the same target.

the particles suffer in their path through the target, and the other comes from the variation in the scattering angle due to the spread in energy carried away by the δ electrons produced in the nucleus-nucleus Rutherford scattering.

The result of the Monte Carlo simulation considering only the angular straggling for the ^{208}Pb-^{208}Pb folding angle distribution for two incident energies $E_{\rm lab}=786.7$ and 1029.9 MeV is shown by the dashed curves in Fig. 4. As can be seen the simulation does not reproduce the width of the experimental distribution, although the insets in Fig. 4 show that the zero degree beam profiles corresponding to the same runs are well reproduced by the simulation. This is explained by the fact that at zero degrees the energy carried away by δ electrons is negligible because of the large impact parameter while at larger angles this effect must be taken into account. We can estimate the fluctuation $\sigma_{Q_{\rm theor}}$ on the energy loss by using Eq. (3):

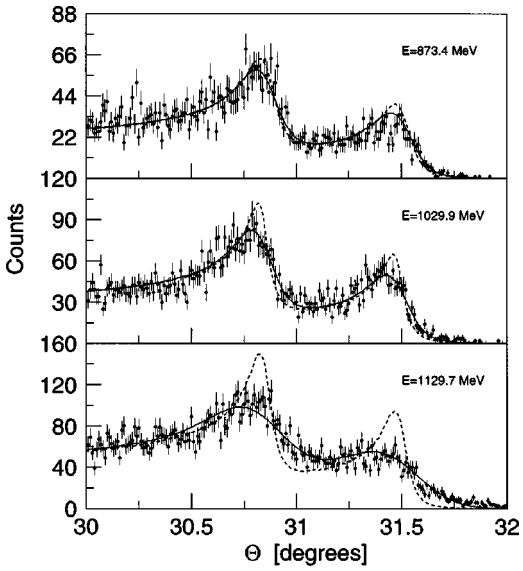

FIG. 5. Spectra of the limiting angles of the ^{208}Pb-^{107,109}Ag scattering. The points represent the experimental data, and the dotted curve is the result of the simulation without energy-loss fluctuation. The solid line is the result of the simulation when this fluctuation is added.

$$\sigma^2_{Q_{\rm theor}}=(\overline{E_{e^-}}+\overline{E_B})^2\sigma^2_{\overline{n}}+\overline{n}^2\sigma^2_{(\overline{E_{e^-}}+\overline{E_B})},$$

where $\sigma_{\overline{n}}\sim\sqrt{\overline{n}}$ is the fluctuation in the number of electrons emitted and $\sigma_{(\overline{E_{e^-}}+\overline{E_B})}$ is the fluctuation in the energy carried away by the electrons. If we make the assumption that all the electrons come from the same atomic shell, this last contribution is reduced to $\sigma_{\overline{E_{e^-}}}$:

$$\sigma^2_{\overline{E_{e^-}}}=\frac{1}{\overline{n}}\int_0^\infty(E_{e^-}-\overline{E_{e^-}})^2\frac{dP}{dE_{e^-}}dE_{e^-}.$$

We obtain therefore

$$\sigma^2_{Q_{\rm theor}}=\overline{n}(\overline{E_{e^-}}+\overline{E_B})^2+\overline{n}\int_0^\infty(E_{e^-}-\overline{E_{e^-}})^2\frac{dP}{dE_{e^-}}dE_{e^-}.$$

The result of this simplified calculation is presented in Table II. This phenomenon can be reproduced in the simulation by introducing a fluctuation $\sigma_{Q_{\rm expt}}$ in the Q value of the Rutherford scattering. When such a fluctuation is intro-

TABLE II. Atomic Q value in MeV for the ^{208}Pb-^{208}Pb and ^{208}Pb-^{107,109}Ag systems. $\sigma_{Q_{\rm expt}}$ is the fluctuation that has to be introduced in the simulation to reproduce the experimental folding angles (^{208}Pb-^{208}Pb) and limiting angles (^{208}Pb-^{107,109}Ag). The expected fluctuation value $\sigma_{Q_{\rm theor}}$ obtained with a simplified calculation for the ^{208}Pb-^{208}Pb scattering is also indicated. The numerical values are all given in MeV.

	^{208}Pb-^{208}Pb			^{208}Pb-^{107,109}Ag	
Energy [MeV]	$\lvert Q\rvert$	$\sigma_{Q_{\rm expt}}$	$\sigma_{Q_{\rm theor}}$	$\lvert Q\rvert$	$\sigma_{Q_{\rm expt}}$
786.7	0.54	0.9	0.47	-	-
873.4	-	-	-	0.9	0.8
1029.9	0.735	1.1	0.68	1.5	1.2
1129.7	-	-	-	1.4	3.2

duced, we obtain the solid line of Fig. 4. The Gaussian fluctuation $\sigma_{Q_{\text{expt}}}$ that gives the best fit to the data is shown in Table II is larger than the expected $\sigma_{Q_{\text{theor}}}$ from our simplified calculation. The fluctuation has the same order of magnitude as the energy loss and it increases with the energy because the number of electrons ejected also increases.

This additional spread in angle is also observed in the shape of the limiting angles of the ^{208}Pb-^{107,109}Ag elastic scattering. Figure 5 presents the spectra of the position-sensitive detector at 30° in the measurement with a natural Ag target. The two peaks observed correspond to the limiting angles of the inverse kinematic scattering of ^{208}Pb on ^{107}Ag and ^{109}Ag. Without angular straggling the number of counts in the spectrum is expected to diverge with a sharp cutoff precisely at the limiting angle. The effect of the angular straggling is to produce a finite peak with a diffuse right side and a shift in the position of the peak with reduction of the peak-to-valley ratio.

In Fig. 5 we present the result of the simulation by taking into account only angular straggling (dashed curve) and straggling plus δ-electron emission (solid curve). The energy loss and the energy loss fluctuation used in the simulation are given in Table II. We observe that the effect of the angular spreading due to the emission of δ electrons increases with energy. For higher energy it has the same order of magnitude as the angular straggling. For this system, we must stress that an additional angular shift due to Coulomb excitation might also be present.

As a final comment we state that the effect of the production of δ electrons on the angular straggling has been observed so clearly in the present experiment primarily because of the use of very thin targets. We expect that for thicker targets the angular straggling in the multiple scattering regime would hide this effect.

VI. CONCLUSION

The angular straggling of a ^{208}Pb beam when transmitted through thin targets of natural Ag or ^{208}Pb was measured around zero degrees by a beam profiler. The shape and width of the distributions are well reproduced by a Monte Carlo simulation of the angular straggling process using the atomic cross section computed from the Thomas-Fermi potential.

We used a ^{208}Pb target to perform measurements of the relative scattering angle between the two lead nuclei around 30°-60° and 45°-45° using kinematic coincidence. For the first time we observed the effect of the production of δ electrons on this scattering angle. This phenomenon, due to the presence of the intense Coulomb field of the two nuclei, induces a change of approximately 0.05° on the centroid of the relative angle of the ^{208}Pb-^{208}Pb scattering, corresponding to an energy loss of about 1 MeV. Because of the direct relation between the mean binding energy of the electrons and the energy loss during the scattering, this experimental setup could represent an original method to measure the mean binding energy of electrons subjected to an intense Coulomb field and ejected during the collision for different systems at different impact parameters.

Finally the present experiment observed the contribution to the angular spreading of the two scattered nuclei due to the fluctuation in the number of electrons emitted and the fluctuation of their binding energy. Monte Carlo simulation of the angular straggling process was not able to explain the entire observed width of the relative angle distributions. However, we found that the angular straggling in addition to the effect of the production of electrons during the scattering to large angles can account for the observed width. This last contribution, shown for the first time in the present work, has the same order of magnitude as the angular straggling in a thin target. In contrast to normal angular straggling due to multiple scattering, this effect occurs in a single scattering.

For precise experiments or estimations, these two new effects, one concerning the absolute scattering angle, the other the straggling, should be taken into account.

Two of the authors (M.E.B. and A.M.-R.) acknowledge partial support from CONACYT-Mexico, through Grant No. 3173E.

[1] G. Hogberg and R. Skoog, *Atomic Collisions in Solids IV* (Gordon and Breach, London, 1972).
[2] F. Hund, Z. Phys. **40**, 742 (1927).
[3] R. S. Mulliken, Phys. Rev. **32**, 186 (1928).
[4] W. M. Coates, Phys. Rev. **46**, 542 (1934).
[5] F. W. Saris, W. F. Van der Weg, H. Tawara, and W. A. Laubert, Phys. Rev. Lett. **28**, 717 (1972).
[6] W. E. Meyerhof, D. L. Clark, C. Stoller, E. Morenzoni, W. Wölfli, F. Folkmann, P. Vincent, P. H. Mokler, and P. Armbruster, Phys. Lett. **70A**, 303 (1979).
[7] W. Greiner, B. Muller, and J. Rafelski, *Quantum Electrodynamics of Strong Fields* (Springer-Verlag, Berlin, 1985).
[8] W. Schaefer, V. Oberacker, and G. Soff, Nucl. Phys. **A272**, 493 (1976).
[9] A. C. C. Villari, W. Mittig, A. Lépine-Szily, R. Lichtenthäler Filho, G. Auger, L. Bianchi, R. Beunard, J. M. Casandjian, J. L. Ciffre, A. Cunsolo, A. Foti, L. Gaudard, C. L. Lima, E. Plagnol, Y. Schutz, R. H. Siemssen, and J. P. Wieleczko, Phys. Rev. Lett. **71**, 2551 (1993).
[10] J. M. Casandjian *et al.* (unpublished).
[11] A. C. C. Villari, W. Mittig, Y. Blumenfeld, A. Gillibert, P. Gangnant, and L. Garreau, Nucl. Instrum. Methods Phys. Res. A **281**, 240 (1989).
[12] J. M. Casandjian, W. Mittig, R. Beunard, L. Gaudard, A. Lépine-Szily, A. C. C. Villari, G. Auger, L. Bianchi, A. Cunsolo, A. Foti, R. Lichtenthäler Filho, E. Plagnol, Y. Schutz, R. H. Siemssen, and J. P. Wieleczko, Nucl. Instrum. Methods Phys. Res. A **334**, 301 (1993).
[13] L. H. Thomas, Proc. Camb. Philos. Soc. **23**, 542 (1927).
[14] E. Fermi, Z. Phys. **48**, 73 (1928).
[15] J. P. Biersack and J. F. Ziegler, Nucl. Instrum. Methods **194**, 93 (1982).
[16] L. Landau and E. Lifchitz, *Mécanique Quantique* (Mir, Moscow, 1974).

[17] J. Lindhard, V. Nielsen, and M. Scharff, Mat. Fys. Medd. K. Dan. Vidensk. Selsk. **36**, 10 (1968).
[18] L. Meyer, Phys. Status Solidi B **44**, 253 (1971).
[19] E. Kankeleit, Nukleonik **25**, 253 (1980).
[20] E. Ditzel (private communication).
[21] G. Soff and U. Muller-Nehler, Phys. Rep. **246**, 101 (1994).
[22] G. Mehler, T. De Reus, J. Reinhardt, G. Soff, and U. Moller, Z. Phys. A **320**, 355 (1985).
[23] E. I. Malkov and I. M. Shmushkevich, Sov. Phys. JETP **12**, 1282 (1961).
[24] J. Reinhardt, G. Soff, and W. Greiner, Z. Phys. A **276**, 285 (1976).
[25] C. A. Bertulani, A. B. Balantekin, and E. Ditzel, Phys. Rev. C **50**, 1104 (1994).
[26] A. Lépine-Szily, J. M. Casandjian, W. Mittig, A. C. C. Villari, R. Lichtenthäler Filho, G. Auger, L. Bianchi, R. Beunard, M. E. Brandan, J. L. Ciffre, A. Cunsolo, A. Foti, L. Gaudard, A. Menchaca-Rocha, N. A. Orr, E. Plagnol, Y. Schutz, R. H. Siemssen, and J. P. Wieleczko, Nucl. Phys. **A538**, 263 (1995).
[27] D. Vetterli, W. Böglin, P. Egelhof, R. Henneck, M. Jaskola, A. Klein, H. Mühry, I. Sick, D. Trautmann, and G. Baur, Nucl. Phys. **A533**, 505 (1991).